Proc. of the 9th Intl. Conf. of Asian Society for Precision Engg. and Nanotechnology (ASPEN 2022)
15–18 November 2022, Singapore. Edited by Nai Mui Ling Sharon and A. Senthil Kumar
doi://10.3850/978-981-18-6021-8_OR-07-0059

Aspects of spindle balancing and consequences on ultra-precision machining

Byron R. Knapp#, Dan Oss and Dave Arneson

Professional Instruments Company, 7800 Powell Road, Hopkins, Minnesota, 55343, USA
Corresponding Author / Email: bknapp@airbearings.com, TEL: +1-952-933-1222

KEYWORDS: Precision balancing, spindle metrology, encoder error correction, torque ripple

Spindle balancing is of critical importance for direct machining optical surfaces—particularly in applications requiring surface form and finish on the nanometer-level. However, various aspects of balancing and its effects on precision machining remain misunderstood including the effects of unbalance on error motions. In this work, the consequences of unbalance vibration on error motion is explored deterministically by measuring error motions of a high speed air bearing spindle as a function of balancing grade. Another critically important issue addressed is torque ripple due encoder eccentricity that creates a vibration masked as unbalance. Incorrect diagnosis of the cause of this "apparent" unbalance vibration and attempts to correct it using balancing can lead to significant errors. Finally, a compensation approach is demonstrated to reduce the apparent unbalance caused by encoder eccentricity using error mapping.

1. Introduction

Despite exhaustive documentation in the literature, balancing and its effect on error motion measurement remains a misunderstood issue. Unbalance at high speeds is a major concern in the manufacture of optical-quality freeform surfaces. It has been asserted that unbalance has little or no effect on surface finish when single-point diamond turning at low speed [1]. However, the majority of precision machining processes (other than the trivial case above) can be negatively impacted by first and higher order harmonics excited in a machine structure by unbalance. This would include high-speed micro-cutting processes such as micro-grinding, raster fly-cutting, and diamond micro-milling resulting in poor surface finish and form errors [2]. Vibration of a machine structure resulting from a rotating unbalance force or moment may lead to many problems, including fundamental (once-per-revolution) axial motion, higher order harmonic motion, inefficient or excessive tool loading leading to accelerated tool wear, and poor dimensional control with changes in speed.

2. Case studies demonstrating the effect of unbalance

2.1 High speed air bearing spindle for micro-machining

An example of a micro-milled lens array is shown in Figure 1. Typically, optics like this are manufactured using single flute diamond ball end-mills with a machine configuration as shown in Figure 2. The diamond end-mill is mounted to the 50,000 RPM air bearing micro-machining spindle discussed in this paper.

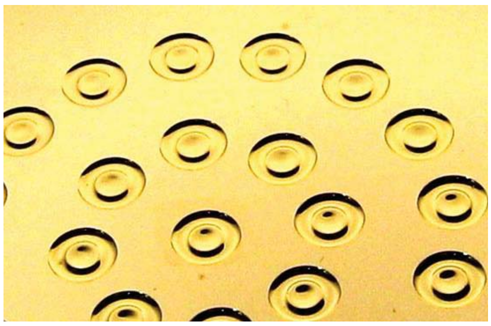

Figure 1. Example of micro-milled lens array.

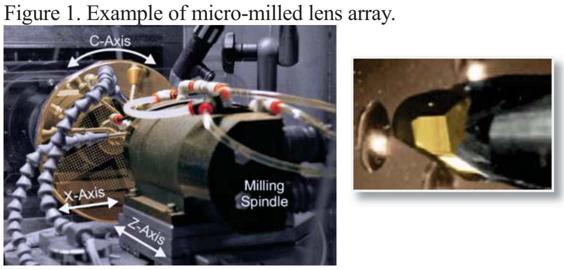

Figure 2. Typical machine configuration with single flute diamond end mill inset.

The water-cooled 50,000 RPM air bearing spindle used to diamond mill the lens array is shown in Figure 3. It incorporates a "captured thrust" groove compensated air bearing between two radial groove compensated air bearing journals. Wide journal bearing spacing provides tilt capacity and stiffness, enabling the use of a smaller diameter thrust and reducing heat generation of the air films. In this spindle, axial and radial air films are 7 µm and spindle temperature is controlled using integrated water-cooling.

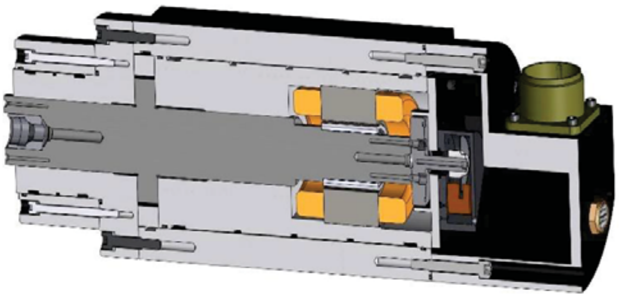

Figure 3. Sectioned view of the ISO 2.25 (50K) high speed air bearing spindle under test.

Figure 4. The residual unbalance is measured with accelerometers and the spindle resting on compliant foam.

The setup for balancing the spindle on foam (extruded polyethylene) is shown in Figure 4. Accelerometers are mounted as close as possible to the two balance correction planes. The spindle encoder is used for angular orientation and balancing software calculates the required mass correction. Use of the encoder index eliminates the need for an external fiducial, such as reflective tape, which can negatively influence balance. Weight corrections on the order of micrograms are removed from M3 setscrews at each balance plane. This minute correction is realized using a buffing wheel to remove weight from the setscrew.

The high-speed air bearing in this work is required to have less than 25 nm axial and radial synchronous error motions through 50,000 RPM. These accuracy requirements demand rigid test hardware and minimization of external influences. This is accomplished using a stiff metrology loop for the capacitive sensors and a flange-mounted spherical artifact bolted to the spindle as shown in Figure 5. The capacitive sensor amplifier incorporates a 15 kHz first-order, low-pass analog filter with linear phase response. The 100-line count encoder triggers the data acquisition system, providing immunity to synchronization errors caused by speed variation.

Figure 5. Setup for error motion testing with capacitive sensor targeting spherical artifact.

To demonstrate the importance of balancing and its effect on nanometer-level error motion, two sets of tests were performed. First, the spindle was balanced to ISO 1940 grade G2.5 and the radial and axial error motions were recorded. Then the balance was improved and the error motions were measured again. The first set of tests simulates balance quality good enough for most machining applications. The magnitude of the rotating unbalance force is calculated for the front and rear balance planes. Residual unbalance is less than the allowable force for ISO 1940 grade G2.5 at all speeds as shown in Figure 6 [3].

The results in Figures 6-9 shown radial and axial results that include spindle error motion, structural error motion, artifact out-of-roundness and misalignment. The radial results in Figure 6 demonstrate less than 25 nm total radial motion over the operating speed range. Axial motion shown in Figure 7 demonstrate less than 25 nm total axial motion up to 40,000 RPM and exceeding the specification at 50,000 RPM due to residual unbalance.

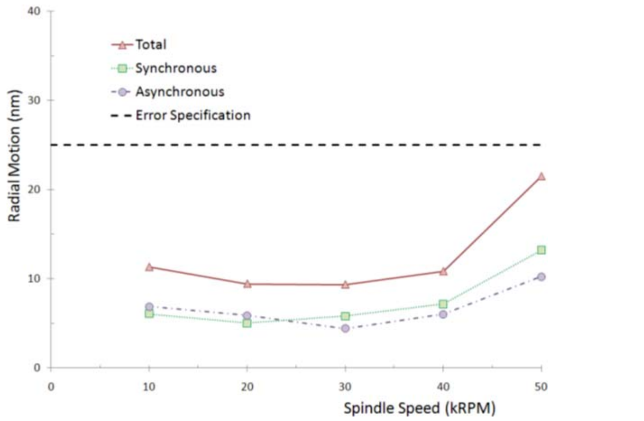

Figure 6. Total radial motion including the artifact is less than 25 nm at all speeds with G2.5 balance.

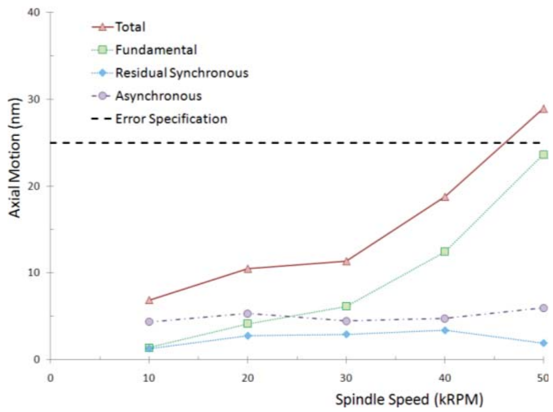

Figure 7. Total axial motion is less than 25 nm up to 40,000 RPM with G2.5 balance. The error motion exceeds the specification at 50,000 RPM due to residual unbalance.

The second set of results demonstrates the effect of a more stringent balance requirement of ISO grade G0.4. Total radial motion shown in Figure 8 is nearly the same as before, due in part, to a stiff metrology loop. However, there is a slight increase in the radial motion at speeds above 40,000 RPM. This result indicates that the shaft is flexing to achieve lower residual unbalance which causes a slight increase in radial error motion [4].

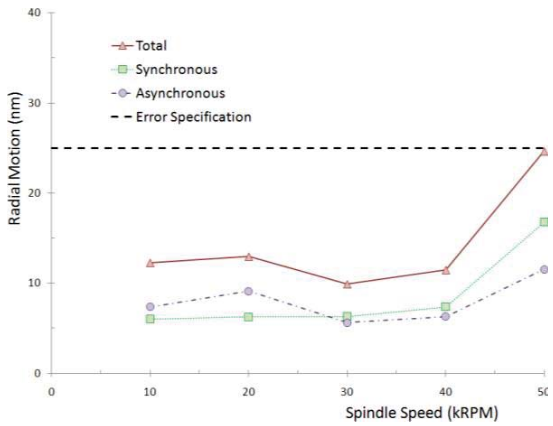

Figure 8. Radial motion with improved balance is less than 25 nm at all speeds.

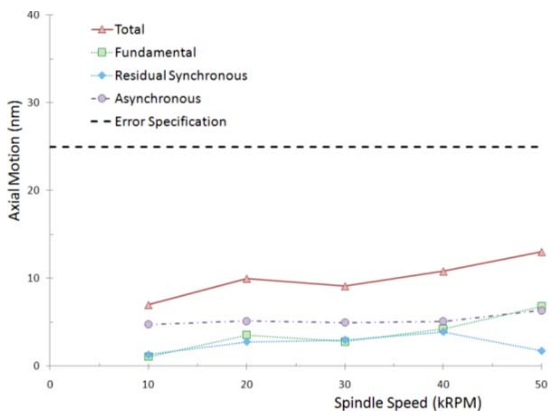

Figure 9. Axial error is dramatically improved with G0.4 balance.

2.2 Torque ripple masked as unbalance

For systems with high dynamic response, torque ripple due to encoder eccentricity can be misinterpreted as unbalance. Attempts to eliminate the vibration due through balancing can lead to unexpected results and increased errors. In this case study, vibration caused by torque ripple due to encoder eccentricity is investigated and potential improvements are suggested.

The air bearing spindle shown in Figure 10 is typical of a spindle used for contact lens turning. It features a frameless brushless servo motor and encoder and is capable of 12,000 RPM with water-cooling. In the presence of encoder eccentricity error, torque ripple from a high bandwidth servo loop (unity gain crossover frequency, fc = 175 Hz) is compared to a lower bandwidth servo loop (fc = 11 Hz). Torque disturbances are introduced at the spindle speed via encoder eccentricity which affect balance. The magnitude and phase of the encoder-related disturbance is dictated by the loop transmissions shown in Figure 3. The unbalance torque disturbance magnitude is proportional to the square of the speed and the phase is dictated by plant dynamics.

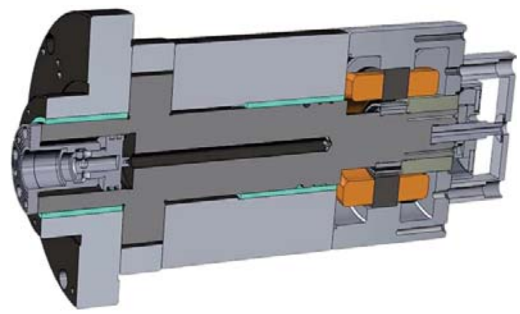

Figure 10. Air bearing spindle to demonstrate the effect of torque ripple.

For the high-bandwidth system shown in Figure 11, vibration levels are below accepted levels at the balancing speed of 66 Hz. However, unacceptable unbalance vibration exists at speeds above and below the 66 Hz balance speed. In the case of the low-bandwidth system, the balance condition below 66 Hz is improved tenfold because the torque disturbance is minimal. The servo loop is not able to track the sinusoidal disturbance caused by encoder eccentricity. Above the balancing speed, the unbalance for the low-bandwidth servo is half as much as the high-bandwidth system. However, the obvious disadvantage of the low-bandwidth servo is the inability to track the desired trajectory resulting in an increased position error.

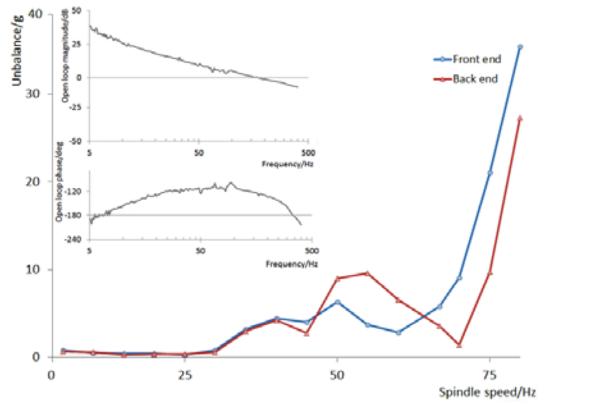

Figure 11 Vibration levels for a high bandwidth servo in the presence of encoder eccentricity. Open loop transmission magnitude and phase shown inset. Balancing speed was 66 Hz.

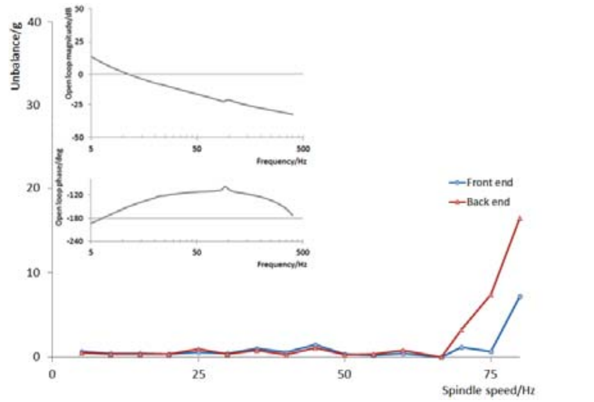

Figure 12. Tenfold improvement in vibration levels for a lower bandwidth servo with identical encoder error.

The corresponding peak-to-peak torque ripple shown in Figure 4 is ten times higher for the high bandwidth system. The servo loop is tracking the sinusoidal disturbance due to eccentricity of the encoder.

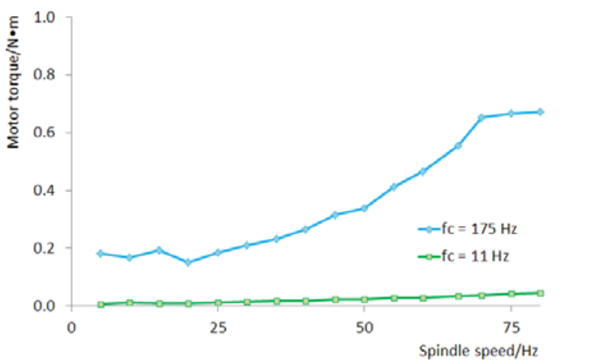

Figure 13. Torque ripple caused by encoder eccentricity for the high and low bandwidth servo systems. The torque ripple is ten times greater for the high bandwidth servo with the same encoder error.

Understanding the cause of vibration in this case requires identification of the disturbance that is masked as unbalance. The magnitude of the vibration due to torque ripple caused by encoder eccentricity is an order of magnitude higher without this error. Therefore, an incorrect diagnosis of the cause of vibration leads to significant errors attempting to eliminate the “apparent” unbalance.

In cases where high bandwidth is required, the torque disturbance must be eliminated. One approach is to uses compensation table to remove the encoder error. This is accomplished using a low bandwidth servo running at a speed well-above the crossover frequency to create the encoder error map. This multistep approach provides precision balance and superb positioning error

3. Conclusions

As demonstrated here, fundamental axial structural motion can be reduced significantly through precision balancing. High resolution balancing is achieved using sensitive accelerometers and balancing on soft foam. A typical installation will likely have more structural compliance than the rigid error motion testbed used in this work. Therefore, the benefits of precision balancing in an actual machine tool will be even more dramatic. In addition, balancing over a wide speed range can only be accomplished by eliminating the torque ripple caused by encoder eccentricity. This is critical to processes sensitive to vibration of the machine structure such as optical surfaces with nanometer-level form tolerances or parts requiring tight dimensional control with changes in speed.

REFERENCES

1. ANSI/ASME B89.3.4. Axes of Rotation; Methods for Specifying and Testing. ASME, 2010.
2. Bryan, J., Clouser, R., and E. Holland, Spindle Accuracy. American Machinist. December 4, 1967; pp. 149-162.
3. ISO 1940-1:2003. Mechanical Vibration – Balance Quality Requirements for Rotors in a Constant (Rigid) State -- Part 1: Specification and Verification of Balance Tolerances. ISO. 2003.
4. Aspects of Flexible Rotor Balancing. 3rd Edition. Schenck Trebel Corporation. Deer Park, New York: 1980.